Innovative Use of Concrete Canvas for Reinforcing Railway Substructures: Enhancing Load-Bearing Capacity and Stability

Balázs Eller[1,2,3], Szabolcs Fischer[1,2,*]

[1]Széchenyi István University
Department of Transport Infrastructure and Water Resources Engineering
Egyetem tér 1, H-9026 Győr, Hungary
{eller.balazs,fischersz}@sze.hu

[2]Széchenyi István University, Vehicle Industry Research Center
Egyetem tér 1, H-9026 Győr, Hungary

[3]University of Pécs
Department of Civil Engineering
Boszorkány út 2, H-7624 Pécs, Hungary
eller.balazs@mik.pte.hu

[*]Corresponding author

Abstract: This study investigates the application of Geosynthetic Cementitious Composite Mats (GCCMs), specifically Concrete Canvas (CC), to reinforce railway substructures. Combining waterproofing, durability, and ease of installation, CC addresses challenges in ballasted railway tracks, such as local failures, moisture, and dynamic forces. The research fills a gap in the literature on CC's dynamic performance and its comparison to geogrids. Experimental methods, including shear box and static plate load tests, revealed that CC increases load-bearing capacity by up to 72% and improves shear resistance through its semi-rigid interlocking mechanism. Robust under dynamic forces, CC ensures stability without deformation. Compared to geogrids, CC offers similar reinforcement, with added benefits like easier hydration and installation. The study concludes that CC is a cost-effective solution for reinforcing railway substructures and improving load distribution and stability. Future research should address environmental impact and integration with advanced materials for enhanced performance and sustainability.

Keywords: GCCM; Concrete Canvas; railway; substructure; load-bearing capacity

1 Introduction

Railway tracks are a vital form of fixed-rail transportation, facilitating efficient land-based travel. They enable the movement of substantial quantities of goods and passengers at relatively high speeds, with low energy consumption and minimal environmental impact – particularly for railways powered by electric traction. For freight transport, rail is especially effective over long distances exceeding 1,000 km, while passenger transport is more relevant for shorter distances, generally under 1,000 km.

Railway operations depend on multidisciplinary collaboration, functioning continuously around the clock. This encompasses a broad range of engineering tasks, such as structural designs, load-bearing capacity, and stability (primarily the domain of civil engineering [1-7]); the configuration and reliable operation of vehicles [8, 9]; logistics and traffic management [10-12]; high-voltage traction and hybrid systems [13,14]; signaling, safety, and telecommunication systems; etc. (The following can also be mentioned subsidiary: transportation and vehicle engineering as well as cognitive mobility [15-18]; etc.).

Railway track structures, whether traditional crushed stone ballast or ballastless designs, consist of two main components: the superstructure and the substructure. This article focuses on thin structural elements at the ballast-substructure interface, analyzing their applicability through laboratory testing, including both static and dynamic assessments.

Adequate drainage and robust subgrade support are crucial for railway structures. Maintenance organizations seek solutions that are multifunctional, cost-effective, and easy to implement, requiring minimal human and mechanical resources while meeting renewal requirements. These solutions enable deferring more costly and extensive interventions, which are often delayed due to financial constraints. Key contributors to track deterioration include inadequate drainage, weak subsoil, and mudding effects. The authors address these challenges through insights from Hungarian State Railways (MÁV) and the Hungarian division of Raaberbahn (ROeEE, Győr-Sopron-Ebenfurth Railways). However, these issues are broadly applicable to railways in other countries as well.

Geosynthetic Cementitious Composite Mats (GCCMs), such as Concrete Canvas, have gained attention in the construction industry [19, 20]. GCCMs are a unique construction material composed of a three-layer structure: a waterproof PVC covering at the bottom, a 3D fiber matrix infilled with a cementitious mixture in the middle, and a textile layer at the top surface [19, 20]. This unique composition allows GCCMs to be easily installed and shaped according to the required form; the authors consider them a promising material for railway substructure reinforcement.

Han et al. [21, 22] studied the influence of 3D spacer fabrics on the drying shrinkage and mechanical properties of Concrete Canvas (CC), highlighting its potential for

use in applications such as slope protection and retaining walls. Niu et al. [23] published that the CC is found to be a promising material for strengthening concrete structures.

Railway track structures are often exposed to track failures, moisture, freeze-thaw cycles in the substructure, and other stresses. From these aspects, the use of GCCMs can provide several benefits, especially in conventional ballasted railway tracks. Compared to traditional materials, GCCMs are easy to install, durable, and can be formed to fit the required substructure geometry [19, 20]. On the other hand, the ability of GCCMs to provide waterproofing gives more advantages for railway applications. This makes them suitable for reinforcing railway substructures or subgrades, particularly in short, local failures.

The flexibility and conformability of GCCMs allow them to be easily integrated with other railway substructure components, such as geotextiles or geogrids, if necessary [24, 25].

While the use of GCCMs in railway substructures is a relatively new concept, the available literature suggests that they have the potential to address several challenges faced by traditional substructure materials.

In addition to the benefits of GCCMs, the professional literature also highlights the potential of other innovative technologies for railway substructure reinforcement. For instance, studies have explored the use of asphalt protection layers [24, 25], recycled aggregates [26, 27], and supplementary cementitious materials or stabilizations [28, 29] to enhance the performance and durability of railway substructures. Integrating these materials with GCCMs could further improve the overall resilience and sustainability of railway infrastructure [24-29]. Moreover, professionals emphasize the importance of considering the environmental impact and sustainability of railway substructure materials. Using waste materials, such as fly ash, slag, and recycled aggregates, can contribute to developing more eco-friendly and resource-efficient railway substructures [26-29].

The results confirmed the material's applicability, but one of the key aspects from a railway perspective is highlighted in this paper. Specifically, the load beneath a railway track is unique. In addition to the dead load, the components of the track structure experience and are subjected to substantial dynamic forces. Given that CC, when bonded, forms a quasi-rigid layer structure, a crucial question arises regarding the material's behavior under dynamic forces. This loading pattern and the material properties cause the ballast stone particles to penetrate the CC, thus working together with the two materials. In addition, the material is resistant to railway loads, and tearing and breakage are not expected under load [30]. Eller and Fischer [31] concluded that the behavior of the CC in this environment is much more similar to that of a semi-rigid structure. Overall, this behavior significantly increases the shear resistance in the railway ballast bed, thanks to the strong interlocking effect [32, 33].

In addition, the rigid layer can affect the distribution of forces, so the authors assumed the possibility of increasing the load-bearing capacity. This assumption was based on the tests of [32, 33], where the load-bearing capacity measurements before and after the multi-level shear box test showed promising results.

According to previous research, a parallel can be found between geogrids and GCCM materials. Therefore, current articles were searched in this professional direction during the literature search. Several studies have already demonstrated the effect of different geogrids on load-bearing capacity. Among the earliest studies relevant to this topic are [34, 35], where the load-bearing capacity measurements were made similarly to those in the current article. It has been confirmed that one or more geogrid layers in the soil can increase the load-bearing capacity of various soil types. These articles are also good references, helping to evaluate the workload of the present work. This can also serve as a direction for designing with CC if someone wants to build permeable and impermeable layers on top of each other in a percolating manner.

2 Materials and Methods

2.1 Materials

The ballast crushed stone used in this test was not the primary focus, as the goal was to assess the total surface loading. However, it is worth noting that the stone was andesite, with grain sizes ranging from 31.5 to 50 mm (the nominal minimum grain size was 31.5 mm, and the maximum was 50 mm) according to the MSZ EN standard [36]. The sample was provided by Colas Északkő Ltd. from the Szob quarry in Hungary.

In this study, the Concrete Canvas (CC) material was sourced from Concrete Canvas Ltd. The dynamic tests were conducted in 2022, while the load-bearing capacity tests took place at the end of 2023 after Concrete Canvas Ltd. had modified the composition of the CC. As a result, the initial tests were performed using CC13 (with the "13" indicating the material's thickness in millimeters), while subsequent tests used the updated CCT3 type. This new type had a reduced maximum thickness of 11 mm due to structural modifications by the manufacturer. Currently, the available types are CCT1, CCT2, and CCT3, with thicknesses of 5, 7, and 11 mm, respectively. These materials are relatively thin compared to the overall structure of a railway track, making them more comparable to geopolymers. Other types of CC, such as CCH and CCX, exist but are less suited to railway loads due to their characteristics.

The granular layers were composed of 0/22 mm crushed stone sourced from a local quarry near Győr, Hungary. The particle size distribution (PSD) was measured to ensure reliable future comparisons, as significant standard deviations had been observed in previous measurements. According to the PSD, the Z0/22 (0/22 mm) material complies with the relevant standard [37]. The measured PSDs are presented in Section 3.1. For the measurement, a multi-level shear box was dismantled into parts for smaller crushed stone thicknesses. With this solution, even two samples can be built at the same time. In these cases, geogrids were not used.

2.2 Methods

In these tests, the increasing effect was measured by different layer structures with and without CC layers. In the tests, steel frame elements with a floor area of 1×1 m were used, which came from the other investigation's multi-level shear box. Due to the dimensions of the box, the test is close to full-scale tests. The cross-section design is seen in Fig. 1.

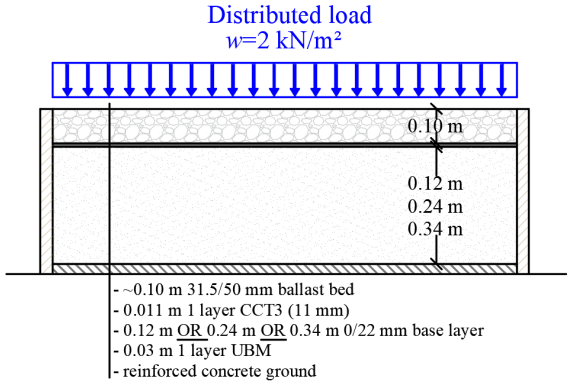

Figure 1
The set-up of the load-bearing capacity test

Under the steel frames, the same UBMs were used to decrease the rigidity of the concrete ground floor, on that 12-24-34 cm thickness of 0/22 mm crushed stone was built in. The last thickness (34 cm) is due to the structural height constraint. Even the thickness of the CC and the crushed stone bedding occupied this surface, but the maximum structural height was 40 cm. In this case, the remaining weight was distributed in a crate. The planned thicknesses were designed according to the available steel frame's height and the accessibility to execute adequate compacting.

The compaction of the protection layer was executed at every 12 cm height.

After the sample was completed, a load-bearing capacity measurement was made. To avoid false results, at the measuring point, the gravel had to be loosened and then recompacted. The compaction method had to be the same procedure. In this

way, the measurement could be re-executed at the same point because only the compaction level has changed and is not significantly changed. The same compaction level was reached with the method of the compaction: same number of repetitions, same length of time.

A 1×1 m CC specimen was laid on the recompacted surface and watered. In this test, it is very significant that the CC layer has to be flat to the surface. After the ballast crushed stone covering, it was watered again.

In order to ensure the correct, necessary fit of the CC and the surface, the authors permanently loaded them with a 15-20 cm crushed stone layer during the binding. The total weight of the stone bed was ~200 kg; thanks to this, it was calculated that the permanent load on the CC was 2 kN/m^2. This permanent loading, while the CC material is curing, is beneficial and helps the stone particle to cement into the CC layer while increasing the stability of the layer.

The stone covering was removed after 7 days of curing. That was the end state of this test. First, the load-bearing capacity was measured on the CC material according to [38]. This means that the static plate load test was performed directly on the CC surface. After the measurement, it can be said that the standard 300 kPa plate loading made no deformation or breakage in the bonded CC material. It is seen in Fig. 2.

Figure 2
Load-bearing capacity measurement on the plan of the CC after measurement

3 Results, Discussion and Proposals

3.1 Results

According to the measurements of Eller et al. [32, 33], it was assumed that load capacity increases with the application of the CC layer. From initial E_2=5.96 MPa, the CC layer affected E_2=12-13 MPa ultimate load-bearing capacity.

After the completed test, the ballast crushed stone bed was removed. In Fig. 3, it is visible that even at this small amount of static load, penetration appears on the CC surface, as shown in Eller et al. [32, 33]. The stone particles were not cemented into the CC layer; instead, they wedged themselves.

Figure 3
The deformed CC surface after w=2 kN/m2 distributed loading

Normally, not much growth is expected from this thin CC layer structure, but if the CC layer is considered a semi-rigid structure (based on the four-point bending measurement of Eller and Fischer [31]), it can be expected that the load will be distributed, which can increase the angle of load distribution. This is the result of the mentioned growth. Following this line of thought, full-scale measurement showed appreciable results. All the results are summarized together.

Table 1 contains the results of the E_2 measurement.

Table 1
Results of the measuring of E_2 *('ult.' means ultimate)*

Layer structure	Average ult. E_2 [MPa]	Average E_2 with CC [MPa]	Average increasing [MPa]	Average effect [%]	Standard deviation [MPa]
SG 14 cm	5.96	12.837	6.88	115.39	0.41
CS 12 cm	20.945	26.12	5.18	28.00	2.72
CS 24 cm	38.44	41.655	3.22	8.62	0.39
CS 34 cm	44.1	47.14	3.04	5.46	4.02
Average			4.58	not relevant	1.89
SG=sandy gravel, CS=0/22 mm crushed stone					

As can be seen in Table 1, noteworthy results were achieved. It should be noted that the authors estimated a relatively large standard deviation for this measurement, too. This was true not only for the measurement with CC but also for the crushed stone sample in itself. The results with and without CC showed a relatively high standard deviation for different layer thicknesses. One of the reasons for this could be the fragmentation of the stone during transport or building. From one point of view, this is a negative experience, on the other hand, it was good to be able to examine even more different starting load-bearing capacity conditions.

The average increase in the different layer structures was between 3.04-6.88 MPa. That means the increasing effect was nearly the same in every case. On the other hand, it must be mentioned that this average increase is not the same as the effect of the real impact. For that, the "Average effect" column provides an answer in Table 1. In the weakest cases, the CC increased by more than 115%.

According to the discussed results, the most straightforward statement is that as the initial load capacity increases, the growth effect also decreases. Although the average reinforcing effect was calculated, due to the variable reinforcing effect, this does not provide an accurate result for drawing more significant conclusions. For this reason, graphical analysis is necessary to determine the reinforcing effect.

In Fig. 4, the full-scale measurement results are shown with and without the CC layer. In addition to the fact that the layer thickness increased linearly, the load-bearing capacity showed logarithmic growth, while in the case of the CC-reinforced layer structure, at the same time, the increasing effect in load-bearing capacity decreased.

In Fig. 5, all four layer structure cases are shown. The weakest case's layer structure and material were different from the new measurements; therefore, other results had to be considered for comparison. For that, the "Average effect [%]" column must be used again from Table 1. Based on the results, it can be said that the increasing effect in load-bearing capacity decreases exponentially with the increase in initial load capacity.

Using the tendency line's equation in Table 2, the expected reinforcement was calculated and attached to round values. Unfortunately, this quasi-unique approach cannot be compared to the materials that are competitors of CC, such as geogrids. Because of this, the load-bearing capacity ratio was calculated by Al-Sumaiday et al. [34] and Indradatna et al. [35]. The load-bearing capacity ratio (*BCR*) represents the ratio of the ultimate load-bearing capacity of reinforced soil to the ultimate load-bearing capacity of unreinforced soil. In this case, the type of subsoil was not taken into account, only the proportions of the reinforcing effect.

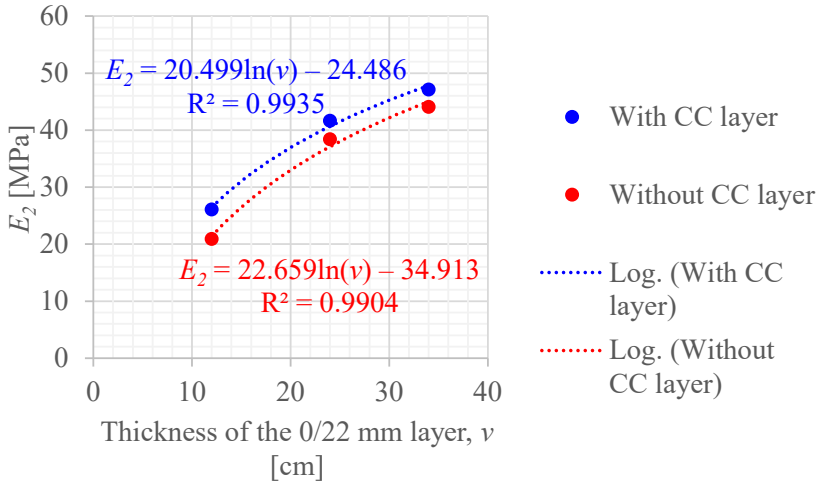

Figure 4
E_2 with and without CC layer

Before the comparison of geogrid and the CC layer examinations were discussed, it had to be mentioned that the tests with geogrids contained more layers of geogrids in the layers structure with soil cover, while the CC was on top, and only one layer was used. Indraratna et al. [35] concluded that the ideal number of layers for geogrid layers with little settlement is three. Al-Sumaiday et al. [34] that their measurements were also made from three layers with biaxial and multi-axial geogrids, too. On the other hand, the method of the test was also different. Despite all this, it can be seen that the average *BCR* is 1.22, 1.23 and 1.63 under different stress peaks and displacements, respectively. Therefore, it can be said that in the case of a low initial load-bearing capacity, the effect of CC is similar to the strengthening effect caused by geogrids installed in several layers.

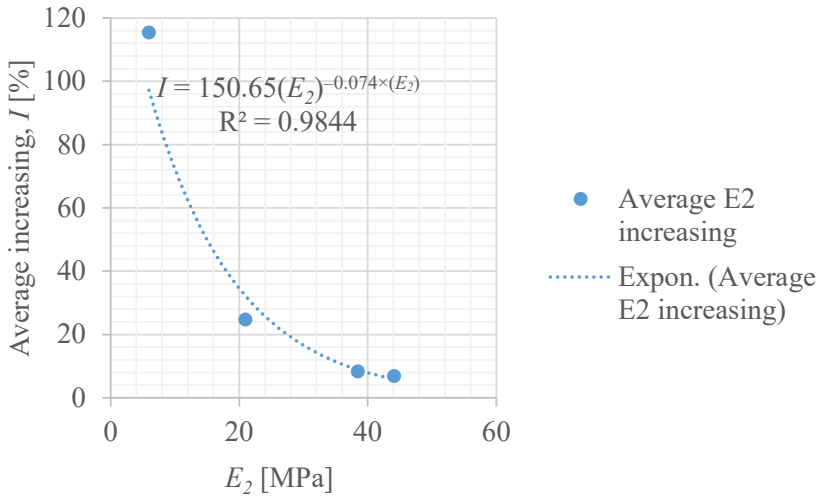

Figure 5
The average increase in E_2 using the CC layer ('expon.' stands for exponential)

Table 2
Estimated reinforcement in percentage

Initial E_2 [MPa]	10	20	30	40	50
Expected increment [%]	71.88	34.29	16.36	7.81	3.72
Expected increment according to the initial E_2 [MPa]	7.19	6.86	4.91	3.12	1.86
Bearing capacity ratio (*BCR*)	1.72	1.34	1.16	1.08	1.04
Estimated E_2 [MPa] after reinforcement	17.19	26.86	34.91	43.12	51.86

Two measurements were made parallel, and the layer orders were always identical, with no variation in material or thickness. However, one sample consistently showed much smaller results. The reason for this was attempted to be determined by taking samples from the core of the 0/22 mm base layer in the middle of the load distribution area. This was important because there could be no difference in the layer structure; the base layer material was the same on both sides. Finally, the PSD curves from the two samples were examined, and this is shown in Fig. 6. The difference can be seen on the weaker side of the samples; the material was more fragmented before or during installation, and less fine content was included. On the weaker the finesses modulus was 6.19; on the stronger side, it was 5.73. On the other hand, it should be mentioned that the standard normal distribution [37] was ensured on both sides (both samples were between the standard border lines), so the different results cannot be considered a serious error, only a minor anomaly. These measurements are equally acceptable.

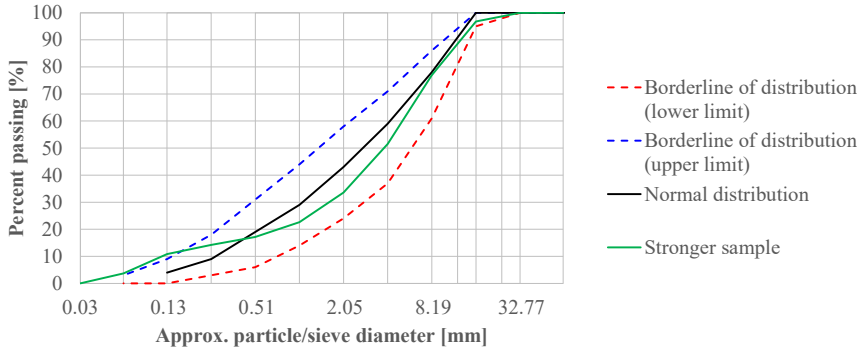

Figure 6

PSD from the load-bearing capacity measurements, samples' Z0/22 protection layer (the applied sieves: 0.032, 0.063, 0.125, 0.25, 0.50, 1, 2, 4, 8, 16, 32, 63 mm) [31]

3.2 Proposals for Structure Formation

3.2.1 Aspects for Determination of Proposals

The proposals are defined for conventional ballasted tracks. The primary consideration was correcting local failures with poor soil conditions and drainage; however, this does not mean it cannot be applied to ballasted high-speed railway lines. From a cost-effectiveness point of view, it would not be worthwhile to cover long sections; renewing short and weak sections could increase the lifetime of the railway track. On the other hand, due to technological considerations, concrete panel high-speed railway tracks were not examined; this solution is effective in the cases of ballasted tracks.

To determine recommendations, it is necessary to clarify the specific advantages of using CC in railway track structures. Previous publications [30-33] have demonstrated the following benefits:

- The material does not break under railway load, and there is no tearing after penetration; thus, the drainage remains adequate even during breakage [30, 31].
- The particles of the ballast bed are cemented into the CC, thus creating a thicker solid layer. Furthermore, the interlocking of the stones increases the shear resistance in the lower 10 cm by 52-57%, thereby increasing the stability of the superstructure [32, 33].

- The CC does not break under the influence of dynamic loading since the fiber reinforcement increases the bending strength of the concrete layer by 81.7% [31].
- The CC increases the load-bearing capacity, as described in Section 3.1.

Conventional ballasted tracks and the ballast-through bridges were examined first. Knowing the advantages, several aspects must be considered during the design of the layer order. These are the problems to be solved, the existing conditions and circumstances, and the production width of the material. With the advantages described above, the following proposals were determined:

1. Solution for water drainage, increasing the stability of the superstructure - closure of the substructure crown at full width, connected with the trench lining, implemented by removing the entire superstructure.
2. Reinforcement of the substructure in the load zone – installation with a screening machine at a width of 4 m.
3. Construction of bridge insulation, improving the stability of the superstructure - installation as bridge insulation.

3.2.2 Construction on Conventional Ballasted Track

When determining the options, we considered a standard ballasted track with the following main parameters:

- 0.5 m ballast thickness, effective ballast thickness min. 0.32 m,
- the breakpoint of the subgrade is 2.0 m from the axle,
- 31.5/50 mm "B" type ballast [36],
- 2.42 m sleeper length,
- 0.6 m sleeper distance,
- 5% subgrade inclination.

The first case is shown in Fig. 7. The design assumes that the subsoil material is weak and water-sensitive. In addition, the previous protection layer is also wet and inadequate. In such cases, complete insulating of the earthwork may be necessary, which can be easily implemented with the CC material. Besides water exclusion, the cover can be connected to the trench cover to create continuous drainage. For that, a proper overlap is necessary. The trench cover can also be built from a material with less thickness, such as 5 mm, since the loads from railways are not considered there. Installing a moisture-absorbing granular layer under the CC layer with a thickness of at least 10 cm is recommended. With this design, in addition to water drainage, it is also possible to increase the stability of the superstructure due to the increase in the shear resistance of the ballast bed. Furthermore, an increase in load-bearing capacity is also possible depending on the initial load-bearing capacity.

The disadvantage of the solution is that it can only be created by completely removing the superstructure. On the other hand, the hydration, in this case, is easier to solve.

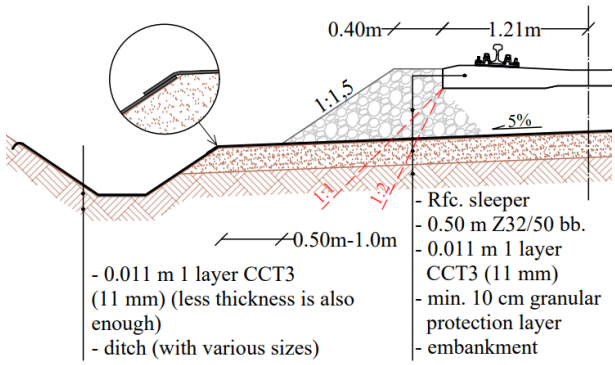

Figure 7

Track renewal by removing the entire superstructure (the embankment is closed from surface waters) – 'Rfc.' means reinforced concrete

The next option is possible if it is not feasible to remove the superstructure completely. The material can be laid under the ballast bed while the screening machine is working. The widest production width of the CC material is 4.0 m, which is ideal for the screening machine. This formation is seen in Fig. 8. The CC can be attached to a screening machine and "pulled" under the crushed stone ballast, similar to the geotextile and/or geogrids. This solution can increase the stability and load-bearing capacity of the superstructure. In addition, although complete drainage is not achieved, this solution reduces the possibility of permanent deflection, thus increasing the service life of the track. With this solution, special attention must be paid to ensuring appropriate hydration. Previous tests have shown that post-watering through the stone subgrade can provide an adequate water supply to achieve the desired consistency. Additional difficulties may arise from the appropriate overlap, but this must be resolved depending on the construction technology.

As described above, it is recommended install a 10 cm layer of moisture-absorbing granular material under the CC layer, while the CC material should be installed directly under the subgrade for the best effect. For optimal results, the CCT3 material is recommended, as it has the most considerable thickness. No further deviation from the standard is required in the railway track structure. As mentioned, the increase in load-bearing capacity improves weak subsoil; however, an increase of more than 10 MPa cannot be achieved based on measurements. For this reason, it is necessary (if possible) to ensure the load-bearing capacity and compactness specified in the standards when using the material.

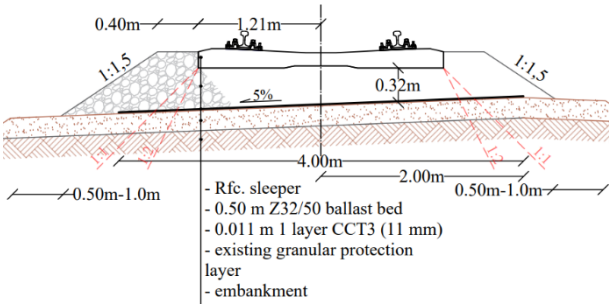

Figure 8

Track renewal involving ballast cleaning and replacement using a screener machine (track stability improvement) – 'Rfc.' means reinforced concrete

3.2.3 Install on Bridges

The following proposal is made for the cases of ballast-through concrete bridges. In these cases, the main concern is the CC's insulating ability. In addition to the insulation, the track's stability is also achieved thanks to the interlocking effect; however, an important aspect is that the track's rigidity will still differ significantly from that of the connecting track section, and the material does not provide additional flexibility. As a result, two roughly identical options have been determined. The first option is when there is no under-ballast mat (UBM), while in the second case, there is one. Regardless, sleepers with under-sleeper pads (USP) are recommended on these sections to increase flexibility.

In Fig. 9, it is seen that the concrete ground of the bridge is continuous, and the CC can lay on it normally, while the ballast particles can be penetrated and cemented into the CC material. The extruded cement material binds the particles located higher up as well.

In Fig. 10, the layer order with UBM is presented. In this case, the UBM is deformed under the dead loads, while the CC will be cured in this state. The interlocking effect will also occur. At this point, the technological process is the same as the version without UBM. Nevertheless, USP is still recommended. Despite the flexibility of the UBM, such a significant movement is not expected due to the flat surface. Therefore, the CC is not likely to break or tear (due to a lack of space). The entire structure works together.

The recommended layer order is shown in Figs. 9 and 10. The solution cannot solve the bridge-railway track transition section. With layer-by-layer installation on the transition sections, even CC material could be used for water drainage and insulation; however, achieving the correct elasticity transition is not possible due to the structural design and rigidity of the material. Based on the points mentioned above and previous experiences, installation in the backfill was not discussed.

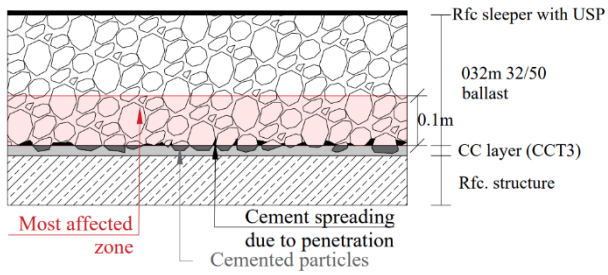

Figure 9
Schematic figure of the setup on an RFC bridge structure (without UBM, with USP sleepers) – 'Rfc.' means reinforced concrete

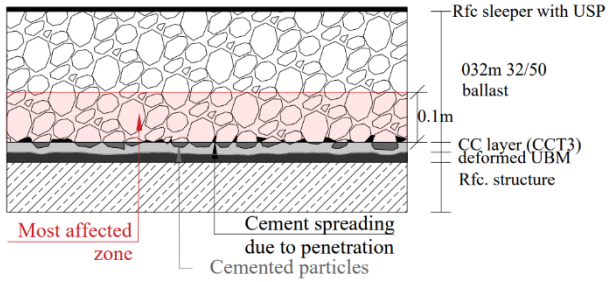

Figure 10
Schematic figure of the set-up on an RFC bridge structure (with UBM, with USP sleepers) – 'Rfc.' means reinforced concrete

Conclusions

The study demonstrated the promising potential of Geosynthetic Cementitious Composite Mats (GCCMs), specifically Concrete Canvas (CC), in reinforcing railway substructures. The research focused on assessing the impact of CC on the load-bearing capacity of railway track layers, revealing substantial improvements in both static and dynamic performance. The results indicated that CC, even as a relatively thin material, can significantly enhance load distribution and increase the stability of the track structure, comparable to the effect of geogrids.

The dynamic tests and load-bearing capacity measurements confirmed that CC provides an effective solution for reinforcing weak subgrades and improving the overall performance of ballasted railway tracks. The material's waterproofing and cementation properties contribute to increased shear resistance and stability, making it an ideal choice for addressing local failures in the railway substructure, especially in areas prone to moisture infiltration or freeze-thaw cycles.

It was found that the application of CC can increase load-bearing capacity by up to 72%, depending on the initial load capacity. From the tests, it is seen, on a 10-50 MPa initial load-bearing capacity scale that the reinforcement value is expected to

be between 1.9 and 7.2 MPa. The higher the initial value, the smaller the strengthening effect. While not much in terms of standard values, this helps when correcting local failures. This supports the statement that the material's installation is cost-effective on short, defective sections rather than on longer, newly constructed sections. On the other hand, it has been proven again that hydration can also work through the ballast crushed stone layer.

Several practical applications were proposed, including its use in repairing local track failures, enhancing drainage, and stabilizing substructures beneath bridges. The study also suggested that the use of CC in conjunction with moisture-absorbing granular materials could further optimize its performance in these applications.

In conclusion, Concrete Canvas presents a viable, cost-effective solution for railway substructure reinforcement at local failures. Its ability to increase load-bearing capacity, improve track stability, and provide waterproofing, combined with its ease of installation, makes it a valuable material for conventional railway infrastructure. Future research should focus on long-term performance and environmental impact assessments to further validate its suitability for widespread adoption in railway engineering.

Future research directions include the extensive laboratory and field applications of Digital Image Correlation (DIC), as used in Eller and Fischer [31], and computer simulations [39-47]. This DIC method is predominantly used in mechanical engineering and materials science and engineering; its use in civil engineering is less well known.

Acknowledgment

This paper was technically supported by the research team entitled "SZE RAIL". Special thanks to Szabolcs Szalai, Majid Movahedi Rad, Imre Fekete, Brigitta Fruzsina Szívós, Hanna Csótár, Vivien Nemes, Dániel Harrach, Gusztáv Baranyai (all from Széchenyi István University), who helped with the execution of laboratory tests. The research was supported by SIU Foundation's project 'Sustainable railways – Investigation of the energy efficiency of electric rail vehicles and their infrastructure'. The publishing of the paper did not receive either financial support, nor financing of the article process charge.

References

[1] Ézsiás, L., Tompa, R., & Fischer, S. (2024) Investigation of the possible correlations between specific characteristics of crushed stone aggregates. *Spectrum of Mechanical Engineering and Operational Research, 1*(1), 10-26

[2] Kuchak, A. T. J., Marinkovic, D., & Zehn, M. (2021) Parametric investigation of a rail damper design based on a lab-scaled model. *Journal of Vibration Engineering & Technologies, 9*, 51-60

[3] Kuchak, A. T. J., Marinkovic, D., & Zehn, M. (2020) Finite element model updating—Case study of a rail damper. *Structural Engineering and Mechanics, 73*(1), 27-35

[4] Kampczyk, A., & Dybeł, K. (2021) The fundamental approach of the digital twin application in railway turnouts with innovative monitoring of weather conditions. *Sensors, 21*(17), 5757

[5] Fischer, S. (2025) Investigation of the settlement behavior of ballasted railway tracks due to dynamic loading. *Spectrum of Mechanical Engineering and Operational Research, 2*(1), 24-46

[6] Fischer, S., Harangozó, D., Németh, D., Kocsis, B., Sysyn, M., Kurhan, D., & Brautigam, A. (2024) Investigation of heat-affected zones of thermite rail weldings. *Facta Universitatis, Series: Mechanical Engineering, 22*(4), 689-710

[7] Alsirawan, R., & Koch, E. (2024) Dynamic analysis of geosynthetic-reinforced pile-supported embankment for a high-speed rail. *Acta Polytechnica Hungarica, 21*(1), 31-50

[8] Lovska, A., Gerlici, J., Dižo, J., & Ishchuk, V. (2023) The strength of rail vehicles transported by a ferry considering the influence of sea waves on its hull. *Sensors, 24*(1), 183

[9] Semenov, S., Mikhailov, E., Kovtanets, M., Sergienko, O., Dižo, J., Blatnický, M., Gerlici, J., & Kostrzewski, M. (2023) Kinematic running resistance of an urban rail vehicle undercarriage: A study of the impact of wheel design. *Scientific Reports, 13*(1), 10856

[10] Volkov, V., Taran, I., Volkova, T., Pavlenko, O., & Berezhnaja, N. (2020) Determining the efficient management system for a specialized transport enterprise. *Naukovyi Visnyk Natsionalnoho Hirnychoho Universytetu, 2020*(4), 185-191

[11] Saukenova, I., Oliskevych, M., Taran, I., Toktamyssova, A., Aliakbarkyzy, D., & Pelo, R. (2022) Optimization of schedules for early garbage collection and disposal in the megapolis. *Eastern-European Journal of Enterprise Technologies, 1*(3(115)), 13-23

[12] Ficzere, P. (2023) The role of artificial intelligence in the development of rail transport. *Cognitive Sustainability, 2*(4), 81

[13] Kampczyk, A., Gamon, W., & Gawlak, K. (2023) Integration of traction electricity consumption determinants with route geometry and vehicle characteristics. *Energies, 16*(6), 2689

[14] Dmitriev, S. V., Morkina, A. Y., Tarov, D. V., Khalikova, G. R., Abdullina, D. U., Tatarinov, P. S., Semenov, A. S., Naimark, O. B., Khokhlov, A. V., & Stolyarov, V. V. (2024) Effect of repetitive high-density current pulses on

plastic deformation of copper wires under stepwise loading. *Spectrum of Mechanical Engineering and Operational Research, 1*(1), 27-43

[15] Zöldy, M., & Baranyi, P. (2023) The cognitive mobility concept. *Infocommunications Journal: A Publication of the Scientific Association for Infocommunications (HTE), (SP)*, 35-40

[16] Zalacko, R., Zöldy, M., & Simongáti, G. (2020) Comparative study of two simple marine engine BSFC estimation methods. *Brodogradnja: An International Journal of Naval Architecture and Ocean Engineering for Research and Development, 71*(3), 13-25

[17] Zöldy, M., Baranyi, P., & Török, Á. (2024) Trends in cognitive mobility in 2022. *Acta Polytechnica Hungarica, 21*(7), 189-202

[18] Zöldy, M., & Zsombók, I. (2019) Influence of external environmental factors on range estimation of autonomous hybrid vehicles. *System Safety: Human-Technical Facility-Environment, 1*(1), 472-480

[19] Anand, S., Manju, R., & Vaardhini, S. (2023) Contemporary research on Concrete Canvas. *International Research Journal of Modernization in Engineering Technology and Science, 5*(3), 3811-3814

[20] Prasanna, C., & Deepak, B. (2019) Concrete Canvas: A multifaceted construction material. *International Journal of Recent Technology and Engineering (IJRTE), 8*(3), 1898-1901

[21] Han, F., Chen, H., Li, X., Bao, B., Lv, T., Zhang, W., & Duan, W. (2015) Improvement of mechanical properties of Concrete Canvas by anhydrite-modified calcium sulfoaluminate cement. *Journal of Composite Materials, 50*(14), 1937-1950

[22] Han, F., Chen, H., Zhang, W., Lv, T., & Yang, Y. (2014) Influence of 3D spacer fabric on drying shrinkage of Concrete Canvas. *Journal of Industrial Textiles, 45*(6), 1457-1476

[23] Niu, J., Xu, W., Li, J., & Liang, J. (2021) Influence of cross-sectional shape on the mechanical properties of Concrete Canvas and CFRP-reinforced columns. *Advances in Materials Science and Engineering, 2021*(1), 5541587

[24] Chango, I. V. L., Assogba, O. C., Yan, M., Ling, X., & Mitobaba, J. G. (2022) Impact assessment of asphalt concrete in geogrid-reinforced-pile-supported embankment during high-speed train traffic. *The Baltic Journal of Road and Bridge Engineering, 17*(2), 135-163

[25] Jadidi, K., Esmaeili, M., Kalantari, M., Khalili, M., & Karakouzian, M. (2020) A review of different aspects of applying asphalt and bituminous mixes under a railway track. *Materials, 14*(1), 169

[26] Kubissa, W., Jaskulski, R., Koper, A., & Supera, M. (2016) High performance concrete with SCM and recycled aggregate. *Key Engineering Materials, 677*, 233-240

[27] Vignesh, G., & Selwyn Babu, J. (2014) Effect of silica fume on properties of high-strength concrete with recycled concrete aggregate. *International Journal of Science and Research (IJSR), 5*(5), 2128-2132

[28] Patel, V. N., Modhera, C. D., Chavda, M. M., & Panseriya, M. M. (2018) Effect of metakaolin on mechanical properties of different grades of concrete including recycled aggregates from C&D waste and ceramic waste. *International Journal of Engineering & Technology, 7*(3.29), 138-142

[29] Sourav Krishnan, A. K., Deepika P., Jasar, V., & Jia Jerin, C. (2023) Improving the mechanical properties of M35 concrete using metakaolin and silica gel. *International Journal for Research in Applied Science and Engineering Technology, 11*(6), 1827-1847

[30] Eller, B., Movahedi Rad, M., Fekete, I., Szalai, S., Harrach, D., Baranyai, G., Kurhan, D., Sysyn, M., & Fischer, S. (2023) Examination of Concrete Canvas under quasi-realistic loading by computed tomography. *Infrastructures, 8*(2), 23

[31] Eller, B., & Fischer, S. (2025) Application of Concrete Canvas for enhancing railway substructure performance under static and dynamic loads. *Facta Universitatis, Series: Mechanical Engineering.* Accepted paper in Online First section. https://doi.org/10.22190/FUME241129002E

[32] Eller, B., Szalai, S., Sysyn, M., Harrach, D., Liu, J., & Fischer, S. (2023) Inner shear resistance increasing effect of Concrete Canvas in ballasted railway tracks. *Naukovyi Visnyk Natsionalnoho Hirnychoho Universytetu, 2023*(2), 64-70

[33] Eller, B., Szalai, S., Sysyn, M., Harrach, D., Liu, J., & Fischer, S. (2024) Advantages of using Concrete Canvas materials in railway track construction. *Naukovyi Visnyk Natsionalnoho Hirnychoho Universytetu, 2024*(1), 50-57

[34] Al-Sumaiday, H., Khalaf, W. D., & Muhauwiss, F. M. (2024) Experimental investigation of bearing capacity of circular and ring footings on geogrid-reinforced cohesionless soils. *Civil and Environmental Engineering, 20*(1), 349-363

[35] Indraratna, B., Rujikiatkamjorn, C., & Salim, W. (2023) *Advanced rail geotechnology-ballasted track* (2nd ed.) CRC Press. London, UK

[36] Hungarian Standards Institute. (2003) *MSZ EN 13450:2003, Aggregates for railway ballast* (33 p.)

[37] Hungarian Standards Institute. (2012) *MSZ EN 933-1:2012, Tests for geometrical properties of aggregates. Part 1: Determination of particle size distribution. Sieving method* (19 p.)

[38] Hungarian Standards Institute. (1989) *MSZ 2509-3:1989, Bearing capacity test on pavement structures. Plate bearing test* (6 p.)

[39] Szalai, S., & Czinege, I. (2017) Digital image analysis of sheet metal testing and forming. *Proceedings of the 15th IMEKO TC10 Workshop on Technical Diagnostics in Cyber-Physical Era,* Budapest, 176-180

[40] Kocsis Szürke, S., Szalai, S., & Lakatos, I. (2020) Battery deformation measurement with DIC technique. *Proceedings of the 21st International Symposium on Electrical Apparatus & Technologies (SIELA),* Bourgas, 91671092

[41] Szalai, S., Harangozó, D., & Czinege, I. (2020) Characterisation of inhomogeneous plastic deformation of AlMg sheet metals during tensile tests. *IOP Conference Series: Materials Science and Engineering, 903*(1), 012023

[42] Kocsis Szürke, S., Dineva, A., Szalai, S., & Lakatos, I. (2022) Determination of critical deformation regions of a lithium polymer battery by DIC measurement and WOWA filter. *Acta Polytechnica Hungarica, 19*(2), 113-134

[43] Szalai, S., & Dogossy, G. (2021) Speckle pattern optimization for DIC technologies. *Acta Technica Jaurinensis, 14*(3), 228-243

[44] Szalai, S., Harangozó, D., & Czinege, I. (2019) Characterisation of diffuse and local necking of aluminium alloy sheets using DIC technique. *Acta Technica Jaurinensis, 12*(3), 191-204

[45] Szalai, S., Eller, B., Juhász, E., Movahedi Rad, M., Németh, A., Harrach, D., Baranyai, G., & Fischer, S. (2022) Investigation of deformations of ballasted railway track during collapse using the Digital Image Correlation Method (DICM). *Reports in Mechanical Engineering, 3*(1), 258-282

[46] Szalai, S., Szívós, B. F., Kocsis, D., Sysyn, M., Liu, J., & Fischer, S. (2024) The application of DIC in criminology analysis procedures to measure skin deformation. *Journal of Applied and Computational Mechanics, 10*(4), 817-829

[47] Kocsis Szürke, S., Szabó, M., Szalai, S., & Fischer, S. (2024) Deformation analysis of different lithium battery designs using the DIC technique. *Energies, 17*(2), 323